Springer

KSME

Journal of Mechanical Science and Technology 30 (6) (2016) 2453~2462
www.springerlink.com/content/1738-494x(Print)/1976-3824(Online)
DOI 10.1007/s12206-016-0505-y

Diagnosing planetary gear faults using the fuzzy entropy of LMD and ANFIS †

Xihui Chen, Gang Cheng*, Hongyu Li and Min Zhang

School of Mechatronic Engineering, China University of Mining and Technology, Xuzhou, 221116, China

(Manuscript Received August 13, 2015; Revised January 5, 2016; Accepted February 21, 2016)

Abstract

The small size, low weight, and large transmission ratio of planetary gear have resulted in large-scale use, low speed, and heavy-duty mechanical systems. Poor working conditions of planetary gear lead to frequent occurrence of faults. A method is proposed for diagnosing faults in planetary gear based on fuzzy entropy of Local mean decomposition (LMD) and Adaptive neuro-fuzzy inference system (ANFIS). The original vibration signal is decomposed into six Product function (PF) components and a residual using LMD. Given that decomposed PF components contain the main fault feature information, fuzzy entropy is used to reflect the complexity and irregularity of each PF component. The fuzzy entropies of each PF component are defined as the input of the ANFIS model, and its parameters and membership functions are adaptively adjusted based on training samples. Finally, fuzzy inference rules are determined, and the optimal ANFIS model is obtained. Testing samples are used to verity the trained ANFIS model. The overall fault recognition rate reaches 88.8%, and the fault recognition rate for gear with wear reaches 96%. Therefore, the proposed method is effective at diagnosing planetary gear faults.

Keywords: Fault diagnosis; Planetary gear; LMD; Fuzzy entropy; ANFIS

1. Introduction

Planetary gear has the characteristics of small size, low weight, and large transmission ratio. These qualities allow for their use in wide scale, low speed, and heavy-duty mechanical systems. However, its working environments are typically unfavorable, which result in faults. Fault diagnosis based on vibration signals is a popular topic in current research. Vibration signals of planetary gear exhibit strong nonlinearity because of the complex structure of planetary gear and the harsh external environment. This feature significantly increases the difficulty of diagnosing faults in planetary gear [1].

Diagnosing faults in planetary gear requires three steps, namely, nonstationary vibration signal processing, effective feature extraction, and fault status recognition [2]. Currently, the most suitable method for processing nonstationary vibration signals is the wavelet transform and Empirical mode decomposition (EMD) [3]. However, the wavelet transform method requires advance determination of the wavelet basis and decomposition layer. Thus, the procedure is not an adaptive decomposition method and suffers from the shortcoming of frequency leakage. The EMD method is an adaptive signal decomposition method that is driven by its own data. However, concerns regarding modal aliasing and endpoint leakage in the EMD process exist [4]. A new time–frequency analysis method proposed by Smith is a Local mean decomposition (LMD) method, which is based on EMD [5]. The vibration signal is decomposed into multiple Product function (PF) components by using the LMD and the PF component is defined as the product of an envelope signal and a Frequency modulation (FM) signal. The envelope signal of each PF component reflects instantaneous amplitude. Instantaneous frequency information can be reflected based on the calculation of the FM signal of each PF component. Compared with EMD, LMD has less decomposition iterative number, endpoint leak is suppressed, and model aliasing problems caused by less and more envelopes are resolved. The fault features of planetary gear can be obtained from each PF component.

The nature of fault feature extraction is that several quantitative values are used to reflect signal status. Traditional fault feature includes time domain and frequency domain features, such as mean, root mean square, and feature frequency profile. However, traditional fault features are only applicable to stationary signals and are inapplicable to nonstationary signals [6]. Entropy theory was originally used in thermodynamics, and researchers have gradually applied feature extraction of nonstationary signals. Singular spectrum, power spectrum, and sample entropy are proposed sequentially [7]. Sample entropy reflects the complexity of the time domain signal from the similarity angle and possibility generated by a new model when dimensions change [8]. In the calculation process of

*Corresponding author. Tel.: +86 516 83591916, Fax.: +86 516 83591916
E-mail address: chg@cumt.edu.cn
† Recommended by Associate Editor Byeng Dong Youn

sample entropy, the similarity of the time domain signals is either similar or dissimilar binary. However, the similarity degree of a real time domain signal sequence is generally vague, which makes accurate determination difficult. Therefore, the similarity of time domain signals should be represented by a vague concept. A combination of fuzzy membership function and sample entropy can be used to measure the complexity and irregularity of time domain signals accurately [9].

Recognizing the status of the planetary gear is key to fault diagnosis once fault features have been extracted, and owing to its development, artificial intelligence technology is being applied in fault diagnosis. Neural network and fuzzy logic are typical examples of artificial intelligence technology [10, 11]. The neural network can learn from the data and has the ability to forecast nonlinear systems. Fuzzy logic, which is applied in many areas, can achieve system inference based on fuzzy language expressions. Casciati [12] used fuzzy logic in the control system for vibration mitigation of space structure. Chong [13] used fuzzy logic to identify and predict output intensity ratio of dye solution of different concentrations. Those studies proved that fuzzy logic is effective in control system, vibration mitigation, and pattern recognition tasks. The combination of neural network and fuzzy logic can fully exploit the learning ability of neural network and inference ability of fuzzy logic, and therefore, Adaptive neuro-fuzzy inference system (ANFIS) was proposed [14]. The proposed ANFIS is constructed from training data and its fuzzy membership functions and fuzzy rules are obtained by self-learning rather than reliance on experience and intuition. Tran [15] proposed a method of diagnosing faults in induction motors based on decision trees and ANFIS, which was used to establish fuzzy rules and identify faults. Zhang [16] proposed a fault classification technique for a neutral non-effectively grounded system using ANFIS, and results showed that the proposed technique was highly accurate and adaptable.

This paper is structured as follows. Sec. 2 establishes a mathematical model for diagnosing planetary gear faults based on the fuzzy entropy of LMD and ANFIS. Sec. 3 presents experiments using DDS comprehensive mechanical fault simulation bench and measurements of vibration signals of planetary gears using acceleration sensors. Sec. 4 discusses the vibration signals of planetary gears that were decomposed into multiple PF components using the LMD method. Fuzzy entropies of each PF component are extracted as fault features. Fault features are encoded as input into the ANFIS model, and faults can be diagnosed and recognized based on the output of the ANFIS model. The last section presents the conclusions.

2. Building model

2.1 Local mean decomposition method

The LMD method uses a moving average to extract pure FM and envelope signals from the original vibration signal, and PF components are obtained by multiplying the FM and envelope signals [17, 18]. The process of LMD is outlined as follows:

(1) All of the local extreme points n_i of signal $x(t)$ are located, and the mean value and envelope estimate of an adjacent local extremum are calculated as follows:

$$\begin{cases} m_i = \dfrac{n_i + n_{i+1}}{2} \\ a_i = \dfrac{n_i - n_{i+1}}{2} \end{cases}, \tag{1}$$

where n_i is the local extremum, m_i is the mean of the local extremum, and a_i is the envelope estimate. Adjacent n_i and m_i are connected by a straight line, and the local mean function $m_{11}(t)$ and envelope estimate function $a_{11}(t)$ are obtained using a moving average.

(2) The result that the original signal subtracts from the local mean function is demodulated as follows:

$$s_{11}(t) = \frac{x(t) - m_{11}(t)}{a_{11}(t)}. \tag{2}$$

(3) A new signal, $s_{11}(t)$, is defined, and the process is repeated until the envelope estimate function $a_{n+1}(t)$ of the FM signal $s_{1n}(t)$ is equal to 1. In practical terms, the end condition is $a_{n+1}(t) \approx 1$.

(4) In the iterative process, the envelope signal is the product of all the envelope estimate functions, as follows:

$$a_1(t) = a_{11}(t)a_{12}(t)...a_{1n}(t) = \prod_{q=1}^{n} a_{1q}. \tag{3}$$

(5) The first PF component is obtained as follows:

$$PF_1(t) = \prod_{q=1}^{n} a_{1q}(t)s_{1n}(t). \tag{4}$$

(6) Residual signal $u_1(t)$ is obtained after the first PF component is extracted from the original signal $x(t)$. $u_1(t)$ is defined as a new signal and the aforementioned steps are repeated k times until $u_k(t)$ becomes a monotonic function. The original signal can be expressed as follows:

$$x(t) = \sum_{j=1}^{k} PF_j(t) + u_k(t). \tag{5}$$

2.2 Fuzzy entropy

Fault features can be extracted from each PF component using fuzzy entropy. Assuming that $PF_i = (x(1), x(2), ..., x(N))$, the following set of vectors can be obtained:

$$A_i = \{x(i), x(i+1), ..., x(i+m-1)\} - u_0(i), \tag{6}$$

where $i = 1, 2, ..., N - m+1$, $u_0(i)$ is the mean value and

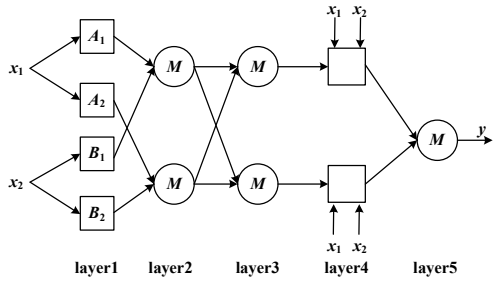

Fig. 1. General structure of ANFIS.

$$u_0(i) = m^{-1}\sum_{j=0}^{m-1} x(i+j) \ .$$

The distance between A_i and A_j is defined as follows [19]:

$$d_{ij}^m(A_i, A_j) = \max\left(\left|A_i(l) - A_j(l)\right|\right) \quad l = 1,2,...,m \ . \tag{7}$$

The fuzzy function is determined as an exponential function, and the similarity degree between row vectors is defined as follows [20]:

$$D_{ij}^m = e^{-(d_{ij}^m/r)^n} \ , \tag{8}$$

where n is the gradient of the exponential function and r is the similar tolerance that represents the width of the exponential function.

A representation function B^m is defined as follows:

$$B^m = \frac{1}{N-m}\sum_{i=1}^{N-m}\left|\frac{1}{N-m-1}\sum_{j=1,j\neq i}^{N-m} D_{ij}^m\right| . \tag{9}$$

Setting $m = m+1$, a set of vectors is constructed based on the original signal. The aforementioned steps are repeated, and the result is obtained as follows:

$$B^{m+1} = \frac{1}{N-m}\sum_{i=1}^{N-m}\left|\frac{1}{N-m-1}\sum_{j=1,j\neq i}^{N-m} D_{ij}^{m+1}\right| . \tag{10}$$

The fuzzy entropy is defined as follows:

$$FE = \ln B^m - \ln B^{m+1} \ . \tag{11}$$

2.3 Adaptive neuro-fuzzy inference system

The general structure of ANFIS, which has two inputs, x_1 and x_2, and one output, y, is shown in Fig. 1, and ANFIS consists of five layers [21, 22].

(1) The first layer is composed of adaptive nodes, which are represented by square nodes. Each node is a membership function of an input variable and can be any suitable parameterized function. The parameters that determine the membership function are called premise parameters, expressed as follows:

$$\begin{cases} O_{1,i} = \mu_{A_i}(x_1), i = 1,2 \\ O_{1,i} = \mu_{B_{i-2}}(x_2), i = 3,4 \end{cases}, \tag{12}$$

where x_1 and x_2 are the system inputs and μ_{A_i} and $\mu_{B_{i-2}}$ are membership functions. A_1 (or B_{i-2}) is the fuzzy set associated with the node.

(2) The second layer is composed of fixed nodes. This layer releases the strength of fuzzy rules. In this layer, the output is the product of membership functions of the input signal, expressed as follows:

$$O_{2,i} = w_i = \mu_{A_i}(x_1)\mu_{B_i}(x_2) \quad i = 1,2 \ . \tag{13}$$

The output of each node represents the activation strength of fuzzy rules.

(3) The third layer is composed of fixed nodes and finds the norm of the strengths of all fuzzy rules. For the *i*-th node, the ratio of the *i*-th rule, w_i, and the sum of all of fuzzy rules, w, is calculated as follows:

$$O_{3,i} = \overline{w}_i = \frac{w_i}{w_1 + w_2} \quad i = 1,2 \ . \tag{14}$$

(4) The fourth layer is composed of adaptive nodes and calculates the output of all fuzzy rules. The output is expressed as follows:

$$O_{4,i} = \overline{w}_i f_i = \overline{w}_i(p_i x_1 + q_i x_2 + r_i) \quad i = 1,2 \ , \tag{15}$$

where $\overline{w}_i$ is the output of the third layer and $\{p_i, q_i, r_i\}$ is the parameter set. The parameters of this layer are called consequent parameters.

(5) The fifth layer is a fixed node that calculates the total output of all input signals, expressed as follows:

$$O_{5,i} = \sum_i \overline{w}_i f_i = \frac{\sum_i w_i f_i}{\sum_i w_i} . \tag{16}$$

In the process of training the ANFIS model, adjusting the premise and consequent parameters is the most critical task, and the adjustment method generally includes the BP algorithm and the algorithm combining BP and least squares. However, a low training speed is a shortcoming of the general BP algorithm, which causes the algorithm to fall easily into the local minimum. Therefore, this study uses numerical optimization techniques and the Levenberg–Marquart algorithm [23] is used to improve the learning speed of the BP algorithm.

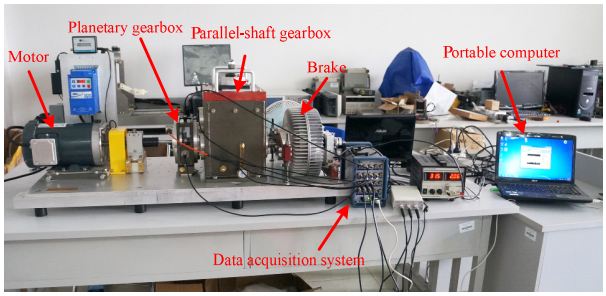

Fig. 2. Fault experiment for planetary gear.

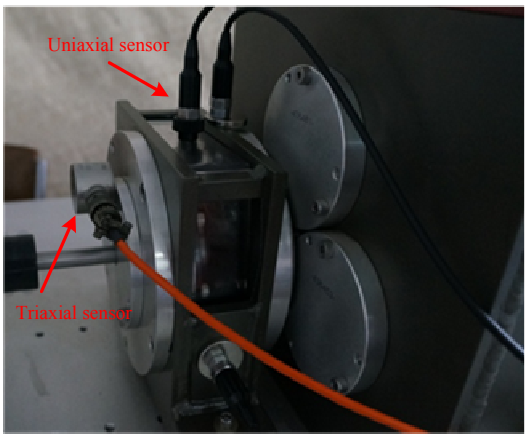

Fig. 3. Layout of acceleration sensors on planetary gearbox.

3. Test equipment and data acquisition

Simulations of planetary gear faults are performed using the comprehensive mechanical fault simulation bench manufactured by Spectra quest in the United States, as shown in Fig. 2. The mechanisms include a programmable control motor, two-stage planetary gearbox, two-parallel-shaft gearbox supported by several rolling bearings, programmable magnetic brake component, data acquisition system and a portable computer. Acceleration sensors, which were manufactured by IMI, are used to measure vibration signals of planetary gear. Fig. 3 shows the layout of acceleration sensors on the planetary gearbox. The data acquisition system is controlled by software installed on the portable computer, and the vibration signals are accurately collected. In this study, the sun gear faults of the second-stage planetary gear are simulated. The setup includes a normal gear, broken gear, gear with a tooth root crack, gear with one missing tooth, and gear with wear, as shown in Fig. 4. The motor output speed is set to 40 Hz, and load is set to 13.5 Nm. The sampling frequency is set to 4200 Hz, and each sample has 8400 data points.

4. Experimental analysis

This study proposes a method for diagnosing planetary gear faults based on fuzzy entropy of LMD and ANFIS. The correctness and effectiveness of the proposed method are tested

Table 1. Basic parameters of two-stage planetary gear.

	First-stage planetary gear			Second-stage planetary gear		
	Sun gear	Planet gear	Ring gear	Sun gear	Planet gear	Ring gear
Teeth	20	40	100	28	36	100

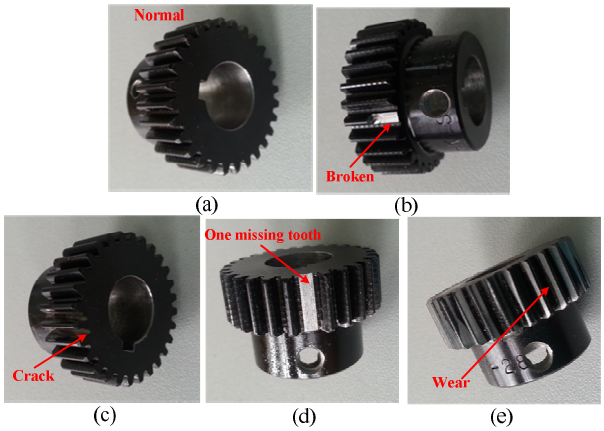

Fig. 4. Common faulty sun gears: (a) Normal gear; (b) broken gear; (c) gear with a tooth root crack; (d) gear with one missing tooth; (e) gear with wear.

by using vibration signals of different gear statuses. Fig. 5 shows the analysis flowchart of the proposed method, and Table 1 presents the basic parameters of the two-stage planetary gear in the comprehensive mechanical fault simulation bench. The feature frequencies of the two-stage planetary gear are determined based on basic parameters and motor output speed, as indicated in Table 2. The vibration signals of five types of gears are shown in Fig. 6.

Given that the structure of the planetary gear is complex, more manufacturing and assembly errors occur. Vibration signals of normal gear have no obvious rules. When a gear fault occurs, the external structure of gear tooth and its stiffness are changed. This change causes the introduction of additional frequency components into the meshing process, and more complex amplitude modulation and FM phenomena are generated. The vibration signal of a broken gear produces periodic shocks, which are shown in the red ellipse in Fig. 6. The shock interval is 0.156 s, which corresponds to a frequency of 6.61 Hz. However, this frequency does not correspond to the feature frequencies given in Table 2 because of the influence of multiple FMs. When a gear loses a tooth, its vibration characteristics change. The amplitude of its time domain signal increases significantly, and more shock components are generated. For gear with wear, each tooth suffers from varying degrees of wear. Therefore, more high-frequency components are generated in the meshing process. Given that the fault degree of gear with a tooth root crack is slight, its time domain signal is not significantly different from that of normal gear. The fault feature information cannot be extracted by analyzing time domain signals of five types of gears, and the gear status cannot be determined.

Table 2. Feature frequencies of two-stage planetary gear.

Motor output frequency	First-stage planetary gear				Second-stage planetary gear			
	Meshing frequency	Feature frequency			Meshing frequency	Feature frequency		
		Sun gear	Planet gear	Ring gear		Sun gear	Planet gear	Ring gear
40 Hz	666.67 Hz	100 Hz	16.67 Hz	20 Hz	145.82 Hz	20.83 Hz	4.05 Hz	5.83 Hz

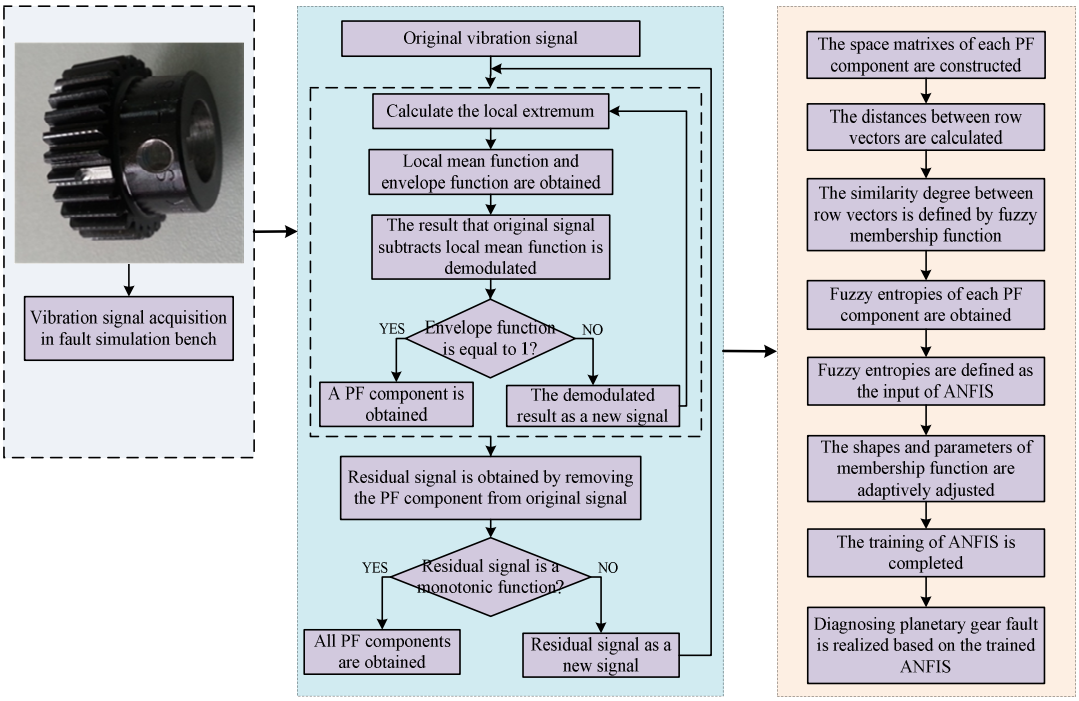

Fig. 5. Experimental analysis flowchart.

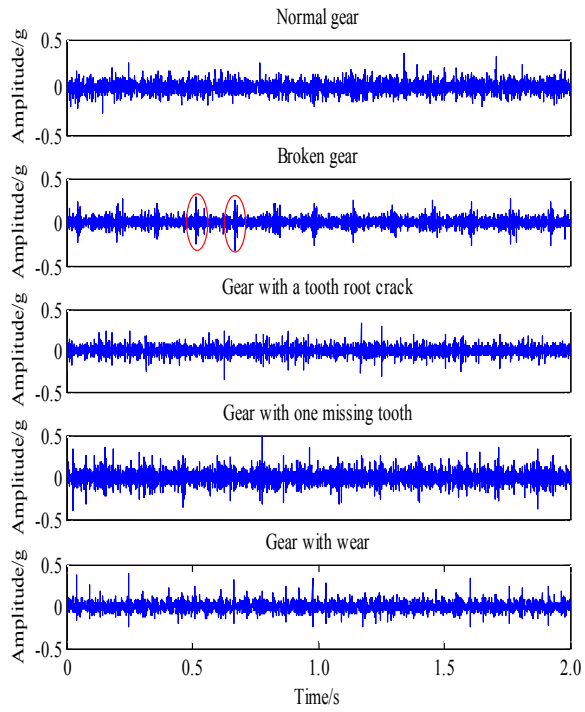

Fig. 6. Vibration signals of five types of gears.

Subsequently, the proposed method for diagnosing planetary gear faults based on the fuzzy entropy of LMD and ANFIS is used to process vibration signals. First, the LMD method decomposes the original vibration signals of five types of gears. Then, a series of PF components is obtained. The vibration signal of the broken gear is selected as an example to show the process of LMD, and the decomposition result of the vibration signal of the broken gear is shown in Fig. 7.

Fig. 7 shows that the original vibration signal is adaptively decomposed into six PF components and a residual signal. The PF1-u components are arranged from high to low frequency. Each PF component contains information of instantaneous amplitude and frequency. When a gear fault occurs, the feature information contained in each PF component changes. Therefore, the effective fault feature information can be extracted by analyzing each PF component. Fuzzy entropy that reflects the complexity and stability of signal is created based on fuzzy membership function and sample entropy theory. Then, a fuzzy description of signal similarity is achieved during the calculating process of fuzzy entropy. The selected fuzzy membership function is required to satisfy the following properties: (1) Continuous to prevent abrupt changes from similarity and (2) convex to ensure maximum self-similarity. Exponential function $D_{ij} = e^{-(d_{ij}/r)^n}$ has been proven better in

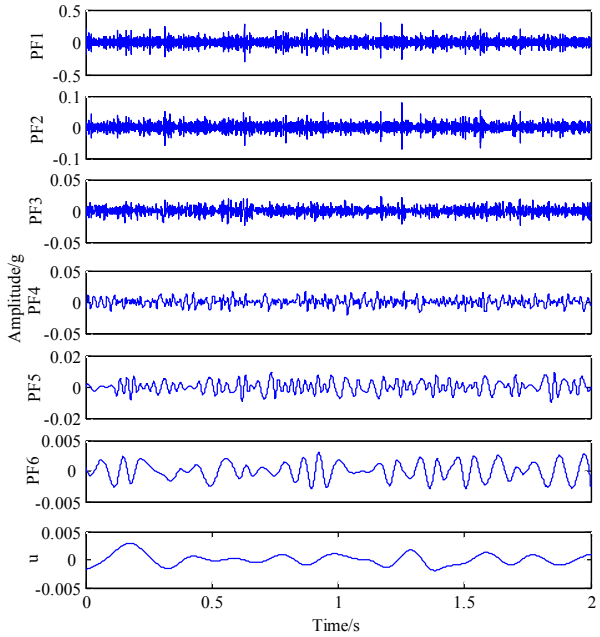

Fig. 7. Decomposition result of the vibration signal of broken gear.

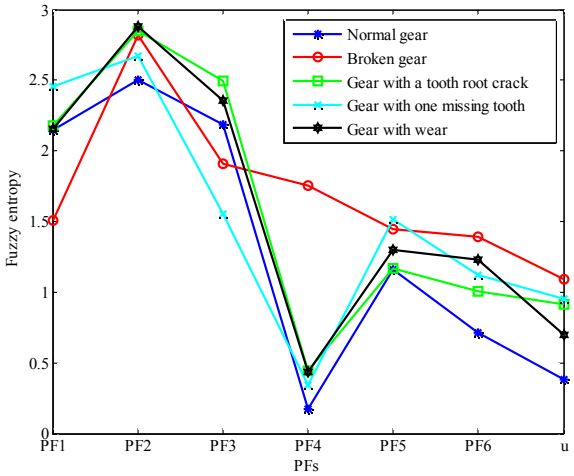

Fig. 8. Fuzzy entropies of each PF component of five types of gears.

acquiring the similarity of the fuzzy measurement of two vectors [24, 25]. However, in the calculating process of fuzzy entropy, similar tolerance r and boundary gradient n of the exponential function need to be set. Similar tolerance r represents the width of the exponential function. r is usually set by the standard deviation of the signal to make the correlation between similar tolerance and time domain signal larger. However, r with a large value would lose more statistical information, whereas r with a small value would cause deviation in statistical probability and increase sensitivity to noise. In general, similar tolerance r usually takes $0.1std$ to $0.2std$, where std is the standard deviation of the original vibration signal.

This study sets similar tolerance to $r = 0.12std$. n is the boundary gradient of similar tolerance and plays a weight role to reflect the similarity among each vector. $n > 1$ represents that more contributions of close vectors to similarity are included and less contribution of the far vectors to similarity is included. $n < 1$ is opposite of $n > 1$. n is recommended to take a smaller integer value, such as 2 or 3, to capture as much detailed information as possible. In this study, n is set as 2. Each PF component includes N data points, and $N = 8400$ in this study. Another parameter, m, needs to be set to construct compared vectors, such as Eq. (6), and the length of the compared vectors to extract fuzzy entropy of each PF component. m that has a small value would cause the compared vectors to contain less feature information, and m that has a large value would cause the number of the compared vectors to become small. In this study, parameter m is obtained based on several experiments. The estimation interval of parameter m is set as [2001, 6000], and the value is taken every 100. Fuzzy entropies of each PF component of five types of gears are calculated under different m values. The essence of feature extraction is that the feature value should allow different faults to be distinguished easily. Thus, the extracted fuzzy entropies of different gears should have certain differences. The absolute value of the difference among the fuzzy entropies of two types of gears is the type–pair separability that represents the degree of difficulty to distinguish those gears. Separabilities of the five types of gears are measured by the summation of all type–pair separabilities. The larger type separability of five types of gears is more conducive to the identification of different gears. After several experiments, parameter m of the fuzzy entropy is determined as 3000. Fig. 8 shows the fuzzy entropies of each PF component of the five types of gears.

Fuzzy entropy combines the fuzzy membership function with the sample entropy; thus, the complexity and irregularity of each PF component could be measured. Fig. 8 indicates that fuzzy entropies of PF2 and PF4-u of normal gear are smallest because the PF components of normal gear are relatively regular and less complex than those of faulty gears. The operating status of a gear changes when a fault occurs, and additional signal components different from that of normal gear are generated during the gear meshing process. This behavior makes the vibration signal more complex. Furthermore, Fig. 8 shows the increases of fuzzy entropies of each PF component of a faulty gear. More significant shock signals are generated because the fault degree of a broken gear is more serious. Given that most of the introduced shock signals have low-frequency characteristics, fuzzy entropies of the PF4-u components of the broken gear are largest. The fuzzy entropies of these gears in the high-frequency band (PF1–PF3) are relatively large because gears with wear or tooth root crack produce more high-frequency signal components during the gear meshing process. As different gears will generate different vibration signals associated with fault types, fuzzy entropies that reflect the complexity and irregularity of each PF component will have differences. Thus, fault features can be successfully quantified and extracted.

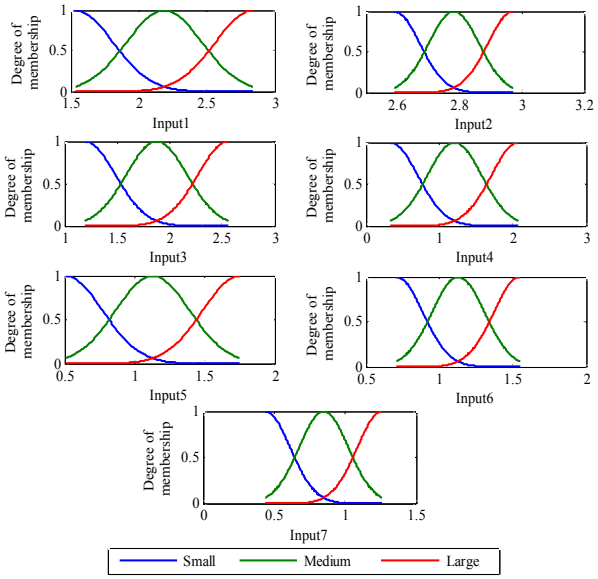

Fig. 9. Initial membership functions of each input of ANFIS.

Classification and recognition are crucial for diagnosing planetary gear faults once fault features have been extracted. ANFIS fully exploits the learning abilities of the neural network and fuzzy expressions of fuzzy logic inference. The parameters of membership functions are adaptively adjusted based on training data during the learning process, and the most suitable fuzzy inference rules are established. Subsequently, ANFIS is used to recognize planetary gear faults. The vibration signals of planetary gears are acquired by the comprehensive mechanical fault simulation bench. Then, training, testing, and checking samples are constructed. Training samples are used to train the ANFIS model. The number of each gear status is 50. Thus, the 5 types of gears gave 250 training samples. Checking samples are used to adjust the auxiliary parameters during the training process. In this study, the number of each gear status is 30, and the 5 five types of gears gave 150 checking samples. The testing samples are used to test and evaluate the ability of the trained ANFIS model to recognize planetary gear faults. Given that the number of each gear status is 50, the 5 types of gears resulted in 250 testing samples. These samples are decomposed using LMD and fuzzy entropies of each PF component are extracted. The fuzzy entropies of each PF component are used as inputs for the ANFIS model. Thus, the ANFIS model has seven inputs. Three Gaussian membership functions are configured for each input. The input is divided into three levels, namely, large, medium, and small. Fig. 9 indicates the initial membership functions for each input of the ANFIS model.

The output of ANFIS is the status of planetary gear. Therefore, to train the ANFIS model, different planetary gears are marked by different numbers, as follows: normal gear—1, broken gear—2, gear with a tooth root crack—3, gear with one missing tooth—4, and gear with wear—5. The parameters and membership functions of the ANFIS model are adaptively

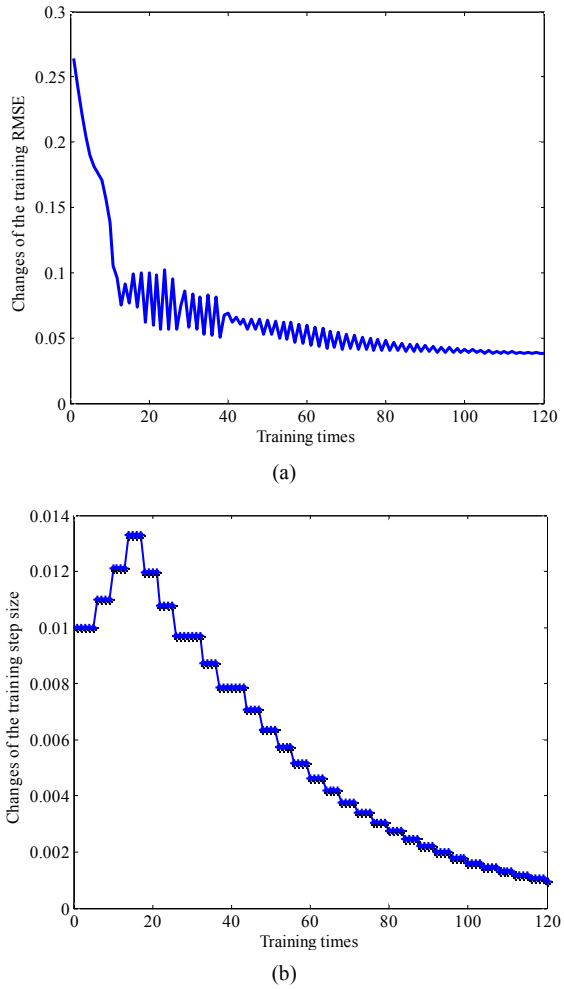

Fig. 10. Changes of the training RMSE and the training step size during the training process: (a) Changes of the training RMSE; (b) changes of the training step size.

adjusted based on the training samples. The Root mean square error (RMSE) is used to evaluate the training process. The training process is controlled by setting the expected RMSE and the training times. In this study, the expected RMSE is set as 0.01, and the training time is set as 120. The initial training step size is set as 0.01, and the training step decreases at a rate of 0.9 and increases at a rate of 1.1. During the training process, the following policies on adjusting the training step size are adopted. When the RMSE decreases four times continuously, the training step is increased. When the RMSE oscillates twice, the training step size is decreased. The changes of the training RMSE are shown in Fig. 10(a), and the changes of the training step size during the training process are shown in Fig. 10(b).

Fig. 10 shows that the training RMSE decreases to 0.05 over 120 training times. The training RMSE is stabilized, and the ANFIS model becomes well trained. When the training process is completed, the parameters and shapes of the membership functions corresponding to each input are adjusted to the most appropriate values. The final adjusted membership

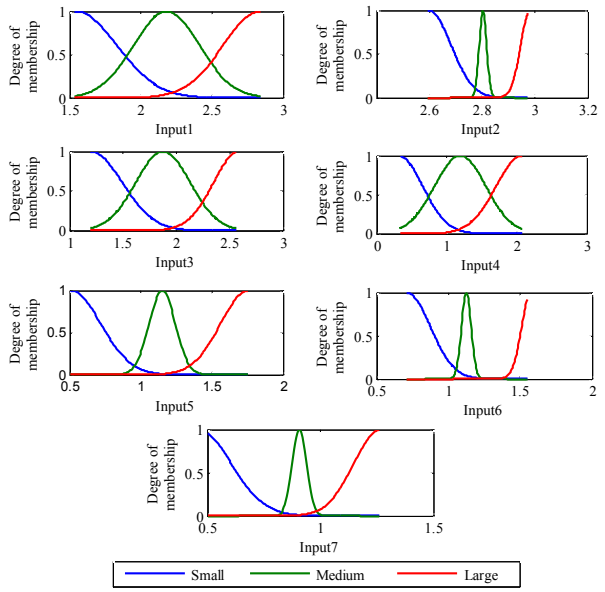

Fig. 11. Final adjusted membership functions of each input of the trained ANFIS.

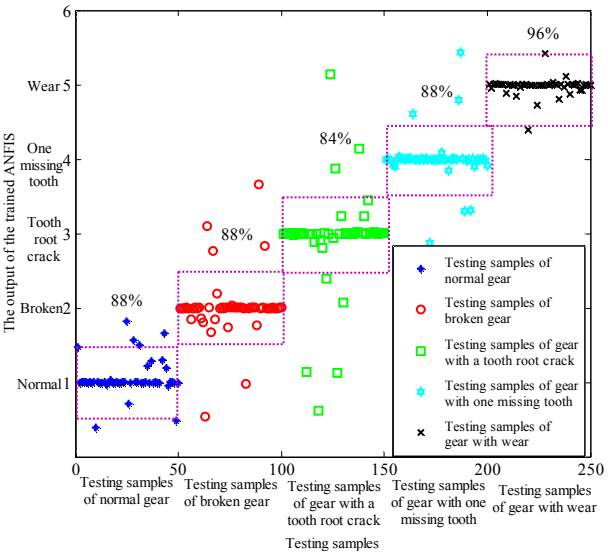

Fig. 12. Output of the trained ANFIS.

functions corresponding to each input are shown in Fig. 11. The comparison between Figs. 9 and 11 indicates that the membership functions of inputs 1, 3, and 4 slightly changed, and the membership functions of inputs 2, 5, 6, and 7 changed more.

Testing samples are used to verify the trained ANFIS model to illustrate the effectiveness of the trained ANFIS model at determining the status of planetary gear. The fuzzy entropies of each PF component of the testing samples are used as the input of the trained ANFIS model, and the output is shown in Fig. 12. Different planetary gears are marked by varied numbers during the training process to distinguish different planetary gear statuses. These numbers are normal gear—1, broken gear—2, gear with a tooth root crack—3, gear with one missing tooth—4, and gear with wear—5. Planetary gear statuses are recognized and diagnosed according to the output of the trained ANFIS model when the testing samples are used as input. If the output is in the interval [0.5, 1.5], then it should be normal gear. If the output is in the interval [1.5, 2.5], then it should be broken gear. If the output is in the interval [2.5, 3.5], then it should be gear with a tooth root crack. If the output is in the interval [3.5, 4.5], then it should be gear with one missing tooth. If the output is in the interval [4.5, 5.5], then it should be gear with wear. If the output is outside of the interval [0.5, 5.5], then the status of the planetary gear cannot be determined. Fig. 12 shows that the trained ANFIS model best recognizes gears with wear, as fault recognition rate reached 96%. The fault recognition rates for normal gears, broken gears, and gears with one missing tooth reached 88%. The fault recognition rate for gears with a tooth root crack reached 84%. The overall fault recognition rate is 88.8%, which showed that the trained ANFIS model performed well. Therefore, the proposed method of diagnosing faults in planetary gear can extract fault features, recognize planetary gear statuses accurately, and is an effective method of diagnosing faults in planetary gear.

5. Conclusion

A method of diagnosing faults in planetary gear that combines fuzzy entropy of LMD and ANFIS is proposed. The vibration signal of the planetary gear is decomposed into a residual and six PF components. Each PF component is constructed by taking the product of envelope and FM signals. The results of LMD contain the feature information of instantaneous frequency and amplitude. For each PF component, fuzzy entropy, which combines fuzzy membership function with sample entropy theory, is used to reflect the complexity and irregularity of the time domain signal. Then, fault features of each PF component are extracted. Fuzzy entropies of each PF component are defined as the input of the ANFIS model, and the marked numbers of different planetary gears are defined as the outputs of the ANFIS model. Initial membership functions of each input are Gaussian functions, and the training process of ANFIS is controlled by the expected RMSE and training times. The parameters and shapes of the membership functions of each input and other ANFIS parameters are adaptively adjusted based on the training samples. Then, the optimal ANFIS model is obtained. Testing samples are used to assess the trained ANFIS model, and the fault recognition rate of gears with wear reached 96%. The fault recognition rates for normal gears, broken gears, and gears with one missing tooth reached 88%, and the recognition rate for gears with a tooth root crack reached 84%. The overall fault recognition rate is 88.8%, which shows that the trained ANFIS model performed well. The results indicated that the proposed method can be used to diagnose faults in planetary gear.

Acknowledgment

This work was supported by a Project Funded by the Priority Academic Program Development of Jiangsu Higher Education Institutions, the Natural Science Foundation of Jiangsu Province (grant number BK20141128) and Fundamental Research Funds for the Central Universities (grant number 2014ZDPY31). This support is gratefully acknowledged.

Nomenclature

A_i : Row vector
$a_{11}(t)$: Envelope estimate function
B^m : Representation function
D_{ij} : Fuzzy function
$d_{ij}(A_i, A_j)$: Distance between A_i and A_j
FE : Fuzzy entropy
m_i : Mean of local extremum
$m_{11}(t)$: Local mean function
N : Number of data points
n_i : Local extremum
$O_{1,i}$: Output of each layer of ANFIS
$PF_1(t)$: First PF component
p_i, q_i, r_i : Parameter set
$s_{1n}(t)$: Frequency modulation signal
$u_1(t)$: Residual signal
w : Output of the third layer
x_1, x_2 : Inputs of ANFIS
$x(t)$: Original vibration signal
y : Output of ANFIS
μ_{A_i} : Membership function

References

[1] F. Chaari, T. Fakhfakh and M. Haddar, Dynamic analysis of a planetary gear failure caused by tooth pitting and cracking, *Journal of Failure Analysis and Prevention*, 6 (2) (2006) 73-78.

[2] Y. G. Lei, J. Lin, Z. J. He and M. J. Zuo, A review on empirical mode decomposition in fault diagnosis of rotating machinery, *Mechanical Systems and Signal Processing*, 35 (1-2) (2013) 108-126.

[3] X. H. Chen, G. Cheng, X. L. Shan, X. Hu, Q. Guo and H. G. Liu, Research of weak fault feature information extraction of planetary gear based on ensemble empirical mode decomposition and adaptive stochastic resonance, *Measurement*, 73 (2015) 55-67.

[4] S. Singh and K. Navin, Combined rotor fault diagnosis in rotating machinery using empirical mode decomposition, *Journal of Mechanical Science and Technology*, 28 (12) (2014) 4869-4876.

[5] Z. P. Feng, M. Liang and F. L. Chu, Recent advances in time-frequency analysis methods for machinery fault diagnosis: a review with application examples, *Mechanical Systems and Signal Processing*, 38 (1) (2013) 165-205.

[6] Y. Zhang, B. W. Li, W. Wang, T. Sun, X. Y. Yang and L. Wang, Supervised locally tangent space alignment for machine fault diagnosis, *Journal of Mechanical Science and Technology*, 28 (8) (2014) 2971-2977.

[7] J. Ye, Fault diagnosis of turbine based on fuzzy cross entropy of vague sets, *Expert Systems with Applications*, 36 (4) (2009) 8103-8106.

[8] D. R. Kong and H. B. Xie, Use of modified sample entropy measurement to classify ventricular tachycardia and fibrillation, *Measurement*, 44 (4) (2011) 653-662.

[9] J. D. Zheng, J. S. Cheng, Y. Yang and S. R. Luo, A rolling bearing fault diagnosis method based on multi-scale fuzzy entropy and variable predictive model-based class discrimination, *Mechanism and Machine Theory*, 78 (16) (2014) 187-200.

[10] J. D. Wu and C. C. Hsu, Fault gear identification using vibration signal with discrete wavelet transform technique and fuzzy-logic inference, *Expert Systems with Applications*, 36 (2) (2009) 3785-3794.

[11] P. K. Mohanty and D. R. Parhi, Navigation of autonomous mobile robot using adaptive network based fuzzy inference system, *Journal of Mechanical Science and Technology*, 28 (7) (2014) 2861-2868.

[12] F. Casciati, M. Domaneschi and L. Faeveelli, Design and implementation of a pointer system controller, *Nonlinear Dynamics*, 36 (2) (2004) 203-215.

[13] S. S. Chong, A. R. A. Aziz, S. W. Harun, H. Arof and S. Shamshirband, Application of multiple linear regression, central composite design, and ANFIS models in dye concentration measurement and prediction using plastic optical fiber sensor, *Measurement*, 74 (2015) 78-86.

[14] K. Salahshoor, M. S. Khoshro and M. Kordestani, Fault detection and diagnosis of an industrial steam turbine using a distributed configuration of adaptive neuro-fuzzy inference systems, *Simulation Modelling Practice and Theory*, 19 (2011) 1280-1293.

[15] V. T. Tran, B. S. Yang, M. S. Oh and A. C. C. Tan, Fault diagnosis of induction motor based on decision trees and adaptive neuro-fuzzy inference, *Expert Systems with Applications*, 36 (2) (2009) 1840-1849.

[16] J. Zhang, X. P. Li and Z. Y. He, Fault classification technique for power distribution network using adaptive network based fuzzy inference system, *Proceedings of the Chinese Society for Electrical Engineering*, 30 (25) (2010) 87-93.

[17] J. D. Sun, Q. Y. Xiao, J. T. Wen and F. Wang, Natural gas pipeline small leakage feature extraction and recognition based on LMD envelope spectrum entropy and SVM, *Measurement*, 55 (9) (2014) 434-443.

[18] W. Y. Liu, W. H. Zhang, J. G. Han and G. F. Wang, A new wind turbine fault diagnosis method based on the local mean decomposition, *Renewable Energy*, 48 (6) (2012) 411-415.

[19] L. Pasi, Feature selection using fuzzy entropy measures with similarity classifier, *Expert Systems with Applications*, 38 (4) (2011) 4600-4607.

[20] J. D. Zheng, J. S. Cheng and Y. Yang, A rolling bearing

fault diagnosis approach based on LCD and fuzzy entropy, *Mechanism and Machine Theory*, 70 (6) (2013) 441-453.

[21] M. S. Ballal, Z. J. Khan, H. M. Suryawanshi and R. L. Sonolikar, Adaptive neural fuzzy inference system for the detection of inter-turn insulation and bearing wear faults in induction motor, *IEEE Transactions on Industrial Electronics*, 54 (2007) 250-258.

[22] A. M. Abdulshahed, A. P. Longstaff, S. Fletcher and A. Myers, Thermal error modeling of machine tools based on ANFIS with fuzzy c-means clustering using a thermal imaging camera, *Applied Mathematical Modeling*, 39 (7) (2015) 1837-1852.

[23] X. X. Wu, X. L. Zhu and H. X. Yang, Application of improved ANFIS in optimization of machining parameters, *Chinese Journal of Mechanical Engineering*, 44 (1) (2008) 199-204.

[24] J. Mongea, C. Gómeza, J. Pozaa, A. Fernándezc, J. Quinteroc and R. Horneroa, MEG analysis of neural dynamics in attention-deficit/hyperactivity disorder with fuzzy entropy, *Medical Engineering and Physics*, 37 (2015) 416-423.

[25] W. Chen, J. Zhuang and W. Yu, Measuring complexity using FuzzyEn, ApEn and SampEn, *Medical Engineering and Physics*, 31 (1) (2009) 61-68.

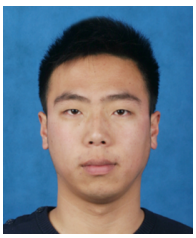

Xihui Chen is currently a doctoral student at the School of Mechatronic Engineering of China University of Mining and Technology in China. His research interests include vibration analysis and fault diagnosis.

Gang Cheng received his M.S. degree from the Chinese Academy of Sciences in 2003 and his Dr. Sc. Tech. degree from China University of Mining and Technology in 2008. Currently, he is a professor of China University of Mining and Technology in China. His research interests include mechanism theory and reliability of electromechanical equipment.

Hongyu Li is currently a postgraduate student at the School of Mechatronic Engineering of China University of Mining and Technology in China. His research interests include vibration analysis and fault diagnosis.

Min Zhang is currently a postgraduate student at the School of Mechatronic Engineering of China University of Mining and Technology in China. His research interests include vibration analysis and fault diagnosis.